



Turing Patterns Induced by Cross-Diffusion in a Predator–Prey System with Functional Response of Holling-II Type

Xiang-Ping Yan¹ · Tong-Jie Yang¹ · Cun-Hua Zhang¹

Received: 6 October 2023 / Accepted: 23 March 2024 / Published online: 16 April 2024
© The Author(s), under exclusive licence to Springer Nature Switzerland AG 2024

Abstract

In this article, a classical predator–prey system with linear cross-diffusion and Holling-II type functional response and subject to homogeneous Neumann boundary condition is considered. The spatially homogeneous Hopf bifurcation curve and Turing bifurcation curve of the constant coexistence equilibrium are established with the help of the linearized analysis. When the bifurcation parameters are restricted to the Turing instability region and near the Turing bifurcation curve, the associated amplitude equations of the original system near the constant coexistence equilibrium are obtained by means of multiple-scale time perturbation analysis. According to the obtained amplitude equations, the stability and classification of spatiotemporal patterns of the original system near the constant coexistence equilibrium are determined. It is shown that the cross-diffusion in the classical predator–prey system plays an important role in formation of spatiotemporal patterns. Also, the theoretical results are verified numerically.

Keywords Predator–prey system · Cross-diffusion · Turing patterns · Amplitude equations · Complicated dynamics

Mathematics Subject Classification 35B35 · 35B40 · 35K57 · 92D40

Supported by the National Natural Science Foundation of China (12261054) and Natural Science Foundation of Gansu Province of China (22JR5RA346).

✉ Xiang-Ping Yan
xpyan72@163.com

¹ Department of Mathematics, Lanzhou Jiaotong University, Lanzhou 730070, Gansu, People's Republic of China

1 Introduction

It is well known that patterns in the nature are ubiquitous and they constitute the colorful world we live. Understanding the formation of patterns is great significant to the research of biological invasion and epidemic diffusion. In his seminal work [23], Turing explained successfully the changes of some animal surface patterns by means of a reaction–diffusion system coupled by two parabolic partial differential equations with homogeneous Neumann boundary conditions. Turing’s findings revealed that different random diffusions of two substances may lead to that a stable spatially uniform steady state loses its stability and then arises the spatially nonuniform patterns. This is called as Turing instability (or diffusion-driven instability). Since Turing’s pioneering work, Turing instability or Turing bifurcation for various reaction–diffusion ecosystems has attracted great interest of lots of researchers [4, 6, 8, 10, 11, 13, 15, 16, 21, 22, 25, 27, 28, 30–32].

In the real world, the interactions among species are various and the one of predator–prey type between two species is of great importance. Assume that there exist only predator and prey species in the same habitat and in the absence of predator species, the growth rate of prey species follows the Logistic growth law and the functional response of predator to prey is of Holling-II type. Then the normalized growth dynamics between two species can be described by the following reaction–diffusion system [20, 29]

$$\begin{cases} \frac{\partial u}{\partial t} = d_{11} \Delta u + u \left(1 - \frac{u}{c}\right) - \frac{muv}{1+u}, & x \in \Omega, t > 0, \\ \frac{\partial v}{\partial t} = d_{22} \Delta v - \theta v + \frac{muv}{1+u}, & x \in \Omega, t > 0, \\ \frac{\partial u}{\partial n} = \frac{\partial v}{\partial n} = 0, & x \in \partial\Omega, t > 0, \end{cases} \quad (1.1)$$

where $\Omega \subset R^N (N \geq 1)$ is a bounded domain with a smooth boundary $\partial\Omega$ and \mathbf{n} is the outside unit normal vector on $\partial\Omega$; the Laplace operator Δ implies that the spatial diffusion of prey and predator species are random and free; the variables $u(x, t)$ and $v(x, t)$ represent respectively the population densities of prey and predator species at space location $x \in \Omega$ and time $t > 0$; $d_{11}, d_{22} > 0$ are separately the diffusion coefficients of prey and predator species; $c > 0$ is the maximum environment carrying capacity of prey species; $\theta > 0$ is the natural death rate of the predator species in the absence of prey species; $m > 0$ is the maximum capture rate of the predator to prey and the function $u/(1+u)$ is the functional response function of predator species to prey species. The homogenous Neumann boundary condition imposed in (1.1) is to guarantee that system (1.1) is self-contained.

Under the assumption that the distribution in space of prey and predator species is homogeneous, namely, in the case when there is no the effect on spatial diffusion, model (1.1) can take the corresponding ordinary differential equation (ODE) model

$$\begin{cases} \frac{du}{dt} = u \left(1 - \frac{u}{c}\right) - \frac{muv}{1+u}, \\ \frac{dv}{dt} = -\theta v + \frac{muv}{1+u}. \end{cases} \quad (1.2)$$

It is easy to reveal that when the condition

(H) $c, m > 0$ and $0 < \theta < \frac{cm}{c+1}$

holds, system (1.2) has the unique positive equilibrium $E_* = (u_*, v_*)$, where

$$u_* = \frac{\theta}{m - \theta}, \quad v_* = \frac{cm - (c + 1)\theta}{c(m - \theta)^2}. \quad (1.3)$$

The asymptotical stability of the unique positive equilibrium E_* of ODE system (1.2) has been investigated extensively by several authors and the following main result has been obtained [7, 12]:

Theorem 1.1 *Assume that the condition (H) holds.*

- (i) *If $(c - 1)/2 < u_* < c$, then the unique positive equilibrium E_* of (1.2) is globally asymptotically stable;*
- (ii) *If $c > 1$ and $0 < u_* < (c - 1)/2$, then the unique positive equilibrium E_* of (1.2) is unstable and (1.2) has a globally asymptotically stable periodic orbit surrounding E_* ;*
- (iii) *When $c > 1$, $u_* = (c - 1)/2$ is the subcritical Hopf bifurcation value of system (1.2) at E_* .*

On the other hand, dynamics of reaction–diffusion system (1.1) has been also investigated deeply by several researchers [20, 29]. For example, under the condition (H), Yi et al. [29] analyzed in detail the spatiotemporal dynamics of (1.1) near the constant coexistence equilibrium E_* including Hopf bifurcation and steady state bifurcation. Peng and Shi [20] further gave some results regarding equilibrium of (1.1) and they obtained that when m is sufficiently large, system (1.1) has no nonconstant positive equilibrium. Meanwhile, it has been found that spatial diffusion in (1.1) does not affect the stability of the constant coexistence equilibrium E_* . Therefore, Turing instability and Turing bifurcation of (1.1) at the constant coexistence equilibrium are impossible and the associated Hopf bifurcation and spatially heterogeneous steady-state solution bifurcation of (1.1) at E_* occur only in the instability regime of the ODE system (1.2). For the dynamics of system (1.1) with delay, see [5, 26]. Also, one can refer to references [1–3, 9] for Hopf bifurcation and steady state bifurcation of the constant coexistence equilibrium in some reaction–diffusion epidemic models.

It should be pointed out that the diffusive system (1.1) can predict more accurately the development of some species than the associated ODE system. However, in modelling (1.1) it is assumed that the diffusion of prey and predator species depends only upon gradients of the concentration of species but not on the spatial distribution of any other species [17]. Therefore, system (1.1) incorporates only the diffusion terms Δu and Δv . In practice, in addition to the self-diffusion in the interior of species, there should also exist cross-diffusion effect among different species [14, 24]. As a result, reaction–diffusion systems with cross-diffusion effect can more practically describe the interactions between different species. Following the idea in [24], the flux of a species should be also induced by a gradient of the other species and according to the Fickian interpretation of the diffusion process, the cross-diffusion term of predator to prey species should take the form $d_{12}v$ and the one of prey to predator species should take the form $d_{21}u$, where $d_{12}, d_{21} \geq 0$ are respectively referred to as the

cross-diffusion coefficients of predator to prey and prey to predator. Based on these considerations and model (1.1), a more reasonable predator–prey system should be described by the following reaction–diffusion system with the linear cross-diffusion

$$\begin{cases} \frac{\partial u}{\partial t} = d_{11} \Delta u + d_{12} \Delta v + u(1 - \frac{u}{c}) - \frac{muv}{1+u}, & x \in \Omega, t > 0, \\ \frac{\partial v}{\partial t} = d_{21} \Delta u + d_{22} \Delta v - \theta v + \frac{muv}{1+u}, & x \in \Omega, t > 0, \\ \frac{\partial u}{\partial n} = \frac{\partial v}{\partial n} = 0, & x \in \partial\Omega, t > 0. \end{cases} \quad (1.4)$$

If we restrict the spatial domain Ω to the planar rectangle domain $\Omega_L = (0, L_x) \times (0, L_y)$ with $L_x, L_y > 0$, then model (1.4) can be read as the following form

$$\begin{cases} \frac{\partial u}{\partial t} = d_{11} \left(\frac{\partial^2 u}{\partial x^2} + \frac{\partial^2 u}{\partial y^2} \right) + d_{12} \left(\frac{\partial^2 v}{\partial x^2} + \frac{\partial^2 v}{\partial y^2} \right) + u(1 - \frac{u}{c}) - \frac{muv}{1+u}, & (x, y) \in \Omega_L, t > 0, \\ \frac{\partial v}{\partial t} = d_{21} \left(\frac{\partial^2 u}{\partial x^2} + \frac{\partial^2 u}{\partial y^2} \right) + d_{22} \left(\frac{\partial^2 v}{\partial x^2} + \frac{\partial^2 v}{\partial y^2} \right) - \theta v + \frac{muv}{1+u}, & (x, y) \in \Omega_L, t > 0, \\ \frac{\partial u}{\partial n} = \frac{\partial v}{\partial n} = 0, & (x, y) \in \partial\Omega_L, t > 0. \end{cases} \quad (1.5)$$

Recently, Wang and Peng [25] investigated numerically the spatiotemporal dynamics of the unique constant coexistence equilibrium E_* of system (1.5) and they found that the linear cross-diffusion effect in (1.5) can induce more complicated spatiotemporal dynamics such as Turing instability and Turing patterns. Since the work in [25] is only numerical but not analytical, the classification and stability of Turing patterns of (1.5) near the unique constant coexistence equilibrium E_* cannot be determined. However, it is more important and interesting to analyze theoretically the classification and stability of Turing patterns of reaction–diffusion systems. Based on these reasons, the main aim of this paper is to explore in detail the classification and stability of Turing patterns of (1.5) near the unique constant coexistence equilibrium E_* .

The layout of this paper is organized as follows. In Sect. 2, we determine the spatially homogeneous Hopf bifurcation curve and Turing bifurcation curve of system (1.5) at the unique constant coexistence equilibrium E_* . In Sect. 3, through multiple-scale time analysis and successive approximations, the amplitude equations of system (1.5) near the unique constant coexistence equilibrium E_* are obtained. In Sect. 4, the existence and stability for different types of patterns arising near the Turing threshold are discussed in detail with the help of the amplitude equations obtained in the previous section. Some numerical simulations are carried out in Sect. 5 to verify the obtained theoretical predictions. Finally, some important conclusions are included also in Sect. 6.

2 Spatially Homogeneous Hopf and Turing Bifurcation Curves

In this section, we obtain the spatial homogeneous Hopf curve and Turing bifurcation curve of the unique constant coexistence equilibrium E_* of system (1.5) and determine

the parameter range in which system (1.5) possesses Turing patterns near the constant coexistence equilibrium E_* .

It is easy to see that under the condition (H), system (1.5) has the unique constant coexistence equilibrium $E_* = (u_*, v_*)$, where u_* and v_* are given by (1.3). The Jacobian matrix of system (1.5) at E_* is

$$J := \begin{pmatrix} a_{11}(\theta) & a_{12}(\theta) \\ a_{21}(\theta) & a_{22}(\theta) \end{pmatrix} = \begin{pmatrix} \frac{\theta[(c-1)m-(c+1)\theta]}{cm(m-\theta)} & -\theta \\ \frac{cm-(c+1)\theta}{cm} & 0 \end{pmatrix}.$$

Let

$$U := \begin{pmatrix} u - u_* \\ v - v_* \end{pmatrix} \text{ and } D := \begin{pmatrix} d_{11} & d_{12} \\ d_{21} & d_{22} \end{pmatrix}.$$

Then the linearized form of system (1.5) at E_* can be written as

$$\begin{cases} \frac{\partial U}{\partial t} = D \left(\frac{\partial^2}{\partial x^2} + \frac{\partial^2}{\partial y^2} \right) U + JU, & (x, y) \in \Omega_L, \\ \frac{\partial U}{\partial n} = 0, & (x, y) \in \partial\Omega_L. \end{cases} \tag{2.1}$$

It follows from [17, 26] that all the eigenvalues of the eigenvalue problem

$$\begin{cases} \left(\frac{\partial^2}{\partial x^2} + \frac{\partial^2}{\partial y^2} \right) u + \mu u = 0, & (x, y) \in \Omega_L, \\ \frac{\partial u}{\partial n} = 0, & (x, y) \in \partial\Omega_L \end{cases}$$

are nonnegative and hence they can be written into k^2 such that they are usually said to be the wavenumbers. For a certain wavenumber k^2 and $0 < \theta < \frac{cm}{c+1}$, define $T_k(\theta)$ and $D_k(\theta)$ by

$$\begin{aligned} T_k(\theta) &= a_{11}(\theta) + a_{22}(\theta) - (d_{11} + d_{22})k^2, \\ D_k(\theta) &= a_{11}(\theta)a_{22}(\theta) - a_{12}(\theta)a_{21}(\theta) - [a_{11}(\theta)d_{22} + a_{22}(\theta)d_{11} - a_{12}(\theta)d_{21} \\ &\quad - a_{21}(\theta)d_{12}]k^2 + (d_{11}d_{22} - d_{12}d_{21})k^4. \end{aligned}$$

Then the characteristic equation of the linear system (2.1) has the form

$$\lambda^2 - T_k(\theta)\lambda + D_k(\theta) = 0. \tag{2.2}$$

If Eq.(2.2) with $k = 0$ has a pair of purely imaginary roots and the associated transversality condition holds, then system (1.5) has a spatially homogeneous Hopf bifurcation at the coexistence equilibrium E_* . When $c > 1$, let

$$\theta_H := \frac{(c-1)m}{c+1}. \tag{2.3}$$

Then one can see that when $c > 1$,

$$T_0(\theta_H) = a_{11}(\theta_H) + a_{22}(\theta_H) = a_{11}(\theta_H) = 0$$

and

$$\begin{aligned} D_0(\theta_H) &= a_{11}(\theta_H)a_{22}(\theta_H) - a_{12}(\theta_H)a_{21}(\theta_H) = -a_{12}(\theta_H)a_{21}(\theta_H) \\ &= \frac{\theta_H[cm - (c + 1)\theta_H]}{cm} = \frac{\theta_H}{c} > 0. \end{aligned}$$

In addition, when $c > 1$ and $k^2 > 0$,

$$T_k(\theta_H) = -(d_{11} + d_{22})k^2 < 0.$$

Therefore, we can obtain that when $c > 1$, the spatially homogeneous Hopf bifurcation curve of (1.5) at E_* is

$$\theta = \theta_H. \tag{2.4}$$

Now we deduce the Turing bifurcation curve of (1.5) at E_* . To achieve this end, we need that the unique positive equilibrium E_* of the ODE system (1.2) is stable, that is,

$$\begin{cases} T_0(\theta) = a_{11}(\theta) + a_{22}(\theta) = \frac{\theta[(c-1)m - (c+1)\theta]}{cm(m-\theta)} < 0, \\ D_0(\theta) = a_{11}(\theta)a_{22}(\theta) - a_{12}(\theta)a_{21}(\theta) = \frac{\theta[cm - (c+1)\theta]}{cm} > 0. \end{cases} \tag{2.5}$$

In fact, we can see easily that (2.5) holds when $c > 1$ and

$$\theta_H < \theta < \frac{cm}{c + 1}. \tag{2.6}$$

Under the condition (2.6), if for some $k > 0$, (2.2) has a root λ_k such that

$$\Re(\lambda_k) = 0, \quad \Im(\lambda_k) = 0,$$

then (1.5) has a Turing bifurcation at E_* . It follows from [22] that under (2.6), if $d_{11}d_{22} - d_{12}d_{21} > 0$, the wave number k^2 takes the critical value $k_T^2 = \sqrt{\frac{a_{11}a_{22} - a_{12}a_{21}}{d_{11}d_{22} - d_{12}d_{21}}}$ and

$$a_{11}d_{22} + a_{22}d_{11} - a_{12}d_{21} - a_{21}d_{12} - 2\sqrt{(d_{11}d_{22} - d_{12}d_{21})(a_{11}a_{22} - a_{12}a_{21})} = 0,$$

then system (1.5) has Turing bifurcation at E_* . Therefore, when (2.6) holds and $d_{11}d_{22} - d_{12}d_{21} > 0$, the Turing bifurcation curve of (1.5) at E_* is given by

$$d_{22} \frac{\theta[(c-1)m - (c+1)\theta]}{cm(m-\theta)} + d_{21}\theta - d_{12} \frac{cm - (c+1)\theta}{cm} - 2\sqrt{(d_{11}d_{22} - d_{12}d_{21}) \frac{\theta[cm - (c+1)\theta]}{cm}} = 0. \tag{2.7}$$

In addition, if (2.6) holds and $d_{11}d_{22} - d_{12}d_{21} > 0$, then the constant coexistence equilibrium E_* of system (1.5) is Turing unstable when

$$d_{22} \frac{\theta[(c-1)m-(c+1)\theta]}{cm(m-\theta)} + d_{21}\theta - d_{12} \frac{cm-(c+1)\theta}{cm} - 2\sqrt{(d_{11}d_{22} - d_{12}d_{21}) \frac{\theta[cm-(c+1)\theta]}{cm}} > 0,$$

and hence the Turing patterns exist. However, when

$$d_{22} \frac{\theta[(c-1)m-(c+1)\theta]}{cm(m-\theta)} + d_{21}\theta - d_{12} \frac{cm-(c+1)\theta}{cm} - 2\sqrt{(d_{11}d_{22} - d_{12}d_{21}) \frac{\theta[cm-(c+1)\theta]}{cm}} < 0,$$

the constant coexistence equilibrium E_* of system (1.5) is locally asymptotically stable.

Summarize the above analysis, we have the following result.

Theorem 2.1 *Suppose that $c > 1$ the condition (2.6) holds, $d_{11}d_{22} - d_{12}d_{21} > 0$ and $\theta = \theta_T(m)$ is defined by Eq. (2.7). Then the constant coexistence equilibrium E_* of system (1.5) is locally asymptotically stable when $\theta > \max\{\theta_H, \theta_T(m)\}$, is Turing unstable as $\theta_H < \theta < \theta_T(m)$ and system (1.5) can undergo a Turing bifurcation at E_* when θ crosses through decreasingly θ_T from up to down. In addition, the constant coexistence equilibrium E_* of system (1.5) is always unstable when $c > 1$ and $0 < \theta < \theta_H$, see Figs. 1 and 2.*

Remark 2.2 Under the conditions (2.6) and $d_{11}d_{22} - d_{12}d_{21} > 0$. If $d_{12} = d_{21} = 0$, then we can see that the left hand side of (2.7) becomes

$$d_{22} \frac{\theta[(c-1)m-(c+1)\theta]}{cm(m-\theta)} - 2\sqrt{d_{11}d_{22} \frac{\theta[cm-(c+1)\theta]}{cm}} < 0.$$

This implies that for all $k^2 \in [0, +\infty)$, all the roots of (2.2) have negative real parts and therefore the constant coexistence equilibrium E_* of system (1.5) is locally asymptotically stable. Thus, the Turing pattern cannot appear in (1.5) and this shows

Fig. 1 Spatially homogeneous Hopf bifurcation and Turing bifurcation curves in m - θ plane of (1.5) at the constant coexistence equilibrium E_*

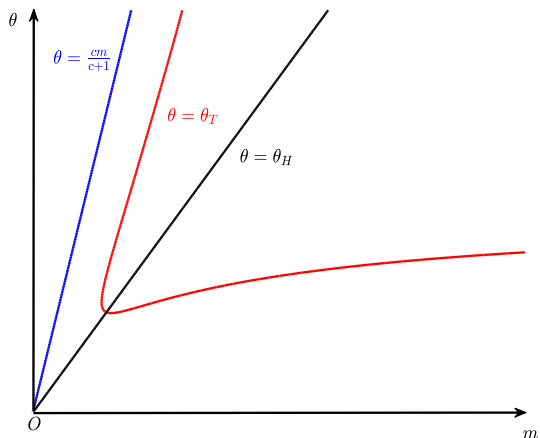
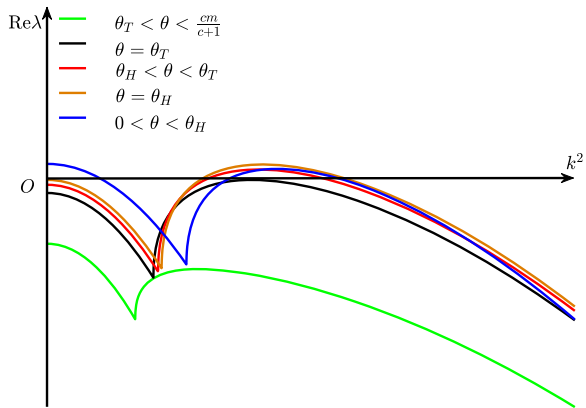


Fig. 2 Graph to relation between $\text{Re}(\lambda)$ of the characteristic Eq. (2.2) and the wavenumber k^2 when m and d_{ij} ($i, j = 1, 2$) are fixed and θ varies



as well that the cross-diffusion plays an important role in the Turing pattern formation of (1.5).

Remark 2.3 If $c > 1$, $0 < \theta < \theta_H$ and $\theta_T(m)$ is defined by the Eq.(2.7), then system (1.5) can bifurcate the spatially heterogeneous steady states from the constant coexistence equilibrium E_* when θ passes through $\theta_T(m)$ from up to down.

3 Amplitude Equations

This section is mainly devoted to obtaining the amplitude equations of system (1.5) at the constant coexistence equilibrium E_* when $0 < \theta_T - \theta \ll 1$ by using multi-scale time analysis.

Assume that $0 < \theta_T - \theta \ll 1$ and let $\hat{u} = u - u_*$, $\hat{v} = v - v_*$. Still denote \hat{u} and \hat{v} by u and v . Then system (1.5) is transformed into the following system

$$\begin{cases} \frac{\partial u}{\partial t} = d_{11} \left(\frac{\partial^2}{\partial x^2} + \frac{\partial^2}{\partial y^2} \right) u + d_{12} \left(\frac{\partial^2}{\partial x^2} + \frac{\partial^2}{\partial y^2} \right) v \\ \quad + (u + u_*) \left(1 - \frac{u+u_*}{c} \right) - \frac{m(u+u_*)(v+v_*)}{1+u+u_*}, & (x, y) \in \Omega_L, t > 0, \\ \frac{\partial v}{\partial t} = d_{21} \left(\frac{\partial^2}{\partial x^2} + \frac{\partial^2}{\partial y^2} \right) u + d_{22} \left(\frac{\partial^2}{\partial x^2} + \frac{\partial^2}{\partial y^2} \right) v \\ \quad - \theta(v + v_*) + \frac{m(u+u_*)(v+v_*)}{1+u+u_*}, & (x, y) \in \Omega_L, t > 0, \\ \frac{\partial u}{\partial n} = \frac{\partial v}{\partial n} = 0, & (x, y) \in \partial\Omega_L, t > 0. \end{cases} \tag{3.1}$$

It is easy to see that the constant coexistence equilibrium E_* of system (1.5) corresponds to zero solution of system (3.1).

Define the real-valued Sobolev space X by

$$X = \left\{ u \in H^2(\Omega_L) \mid \frac{\partial u}{\partial n} = 0, (x, y) \in \partial\Omega_L \right\}$$

and

$$\begin{cases} f(u, v) = (u + u_*)(1 - \frac{u+u_*}{c} - \frac{m(u+u_*)(v+v_*)}{1+u+u_*}), \\ g(u, v) = -\theta(v + v_*) + \frac{m(u+u_*)(v+v_*)}{1+u+u_*}. \end{cases}$$

Then system (3.1) can be further expressed in view of Taylor expansion of $f(u, v)$ and $g(u, v)$ at $(0, 0)$ as

$$\frac{\partial U}{\partial t} = L(\theta)U + N(\theta; U, U), \tag{3.2}$$

where $U = (u, v)^T \in X^2$, the linear operator $L(\theta) : X^2 \rightarrow [L^2(\Omega)]^2$ is defined by

$$L(\theta) = \begin{pmatrix} a_{11}(\theta) + d_{11} \left(\frac{\partial^2}{\partial x^2} + \frac{\partial^2}{\partial y^2} \right) & a_{12}(\theta) + d_{12} \left(\frac{\partial^2}{\partial x^2} + \frac{\partial^2}{\partial y^2} \right) \\ a_{21}(\theta) + d_{21} \left(\frac{\partial^2}{\partial x^2} + \frac{\partial^2}{\partial y^2} \right) & a_{22}(\theta) + d_{22} \left(\frac{\partial^2}{\partial x^2} + \frac{\partial^2}{\partial y^2} \right) \end{pmatrix}$$

with

$$\begin{aligned} a_{11}(\theta) &= \frac{\theta[(c - 1)m - (c + 1)\theta]}{cm(m - \theta)}, & a_{12}(\theta) &= -\theta, & a_{21}(\theta) &= \frac{cm - (c + 1)\theta}{cm}, \\ a_{22}(\theta) &= 0, \end{aligned}$$

and the nonlinear mapping $N(\theta; \cdot, \cdot) : X^2 \times X^2 \rightarrow [L^2(\Omega)]^2$ is given by

$$\begin{aligned} N(\theta; U, U) &= \left(\begin{aligned} &\frac{f_{uu}(\theta)}{2}u^2 + f_{uv}(\theta)uv + \frac{f_{vv}(\theta)}{2}v^2 + \frac{f_{uuu}(\theta)}{3!}u^3 + \frac{f_{uuv}(\theta)}{2}u^2v + \frac{f_{uvv}(\theta)}{2}uv^2 + \frac{f_{vvv}(\theta)}{3!}v^3 \end{aligned} \right), \\ &= \left(\begin{aligned} &\frac{g_{uu}(\theta)}{2}u^2 + g_{uv}(\theta)uv + \frac{g_{vv}(\theta)}{2}v^2 + \frac{g_{uuu}(\theta)}{3!}u^3 + \frac{g_{uuv}(\theta)}{2}u^2v + \frac{g_{uvv}(\theta)}{2}uv^2 + \frac{g_{vvv}(\theta)}{3!}v^3 \end{aligned} \right), \end{aligned} \tag{3.3}$$

here

$$\begin{aligned} f_{uu}(\theta) &= \frac{2(c - 1)m^2 - 2(2c + 1)m\theta + 2(c + 1)\theta^2}{cm^2}, & f_{uv}(\theta) &= -\frac{(m - \theta)^2}{m}, \\ f_{vv}(\theta) &= 0, \end{aligned}$$

$$\begin{aligned} f_{uuu}(\theta) &= -\frac{6(m - \theta)^2[c(m - \theta) - \theta]}{cm^3}, & f_{uuv}(\theta) &= \frac{2(m - \theta)^3}{m^2}, & f_{uvv}(\theta) &= 0, \\ f_{vvv}(\theta) &= 0, \end{aligned}$$

$$g_{uu}(\theta) = -\frac{2(m - \theta)[c(m - \theta) - \theta]}{cm^2}, \quad g_{uv}(\theta) = \frac{(m - \theta)^2}{m}, \quad g_{vv}(\theta) = 0,$$

$$g_{uuu}(\theta) = \frac{6(m - \theta)^2[c(m - \theta) - \theta]}{cm^3}, \quad g_{uuv}(\theta) = -\frac{2(m - \theta)^3}{m^2}, \quad g_{uvv}(\theta) = 0, \\ g_{vvv}(\theta) = 0.$$

Since the calculation is only limited to the case when $0 < \theta_T - \theta \ll 1$, it follows that θ can be expressed as

$$\theta - \theta_T = \epsilon\theta_1 + \epsilon^2\theta_2 + O(\epsilon^3), \tag{3.4}$$

where ϵ is a very small positive number. Making use of the expansion (3.4), U can be expanded as the following power series

$$U = \begin{pmatrix} u \\ v \end{pmatrix} = \epsilon \begin{pmatrix} u_1 \\ v_1 \end{pmatrix} + \epsilon^2 \begin{pmatrix} u_2 \\ v_2 \end{pmatrix} + \epsilon^3 \begin{pmatrix} u_3 \\ v_3 \end{pmatrix} + O(\epsilon^4). \tag{3.5}$$

Thus the nonlinear mapping $N(\theta; U, U)$ defined by (3.3) has the form

$$N(\theta; U, U) = \epsilon^2 N_2(\theta_T) + \epsilon^3 [N_{31}(\theta_T) + \theta_1 N_{32}(\theta_T)] + O(\epsilon^4), \tag{3.6}$$

where

$$N_2(\theta_T) = \begin{pmatrix} \frac{f_{uu}^*}{2} u_1^2 + f_{uv}^* u_1 v_1 + \frac{f_{vv}^*}{2} v_1^2 \\ \frac{g_{uu}^*}{2} u_1^2 + g_{uv}^* u_1 v_1 + \frac{g_{vv}^*}{2} v_1^2 \end{pmatrix},$$

$$N_{31}(\theta_T) = \begin{pmatrix} f_{uu}^* u_1 u_2 + f_{uv}^* (u_1 v_2 + u_2 v_1) + f_{vv}^* v_1 v_2 + \frac{f_{uuu}^*}{3!} u_1^3 + \frac{f_{uuv}^*}{2} u_1^2 v_1 + \frac{f_{uvv}^*}{2} u_1 v_1^2 + \frac{f_{vvv}^*}{3!} v_1^3 \\ g_{uu}^* u_1 u_2 + g_{uv}^* (u_1 v_2 + u_2 v_1) + g_{vv}^* v_1 v_2 + \frac{g_{uuu}^*}{3!} u_1^3 + \frac{g_{uuv}^*}{2} u_1^2 v_1 + \frac{g_{uvv}^*}{2} u_1 v_1^2 + \frac{g_{vvv}^*}{3!} v_1^3 \end{pmatrix},$$

as well as

$$N_{32}(\theta_T) = \begin{pmatrix} \frac{f_{uuv}^*}{2} u^2 + f_{uv\theta}^* uv + \frac{f_{vv\theta}^*}{2} v^2 \\ \frac{g_{uuv}^*}{2} u^2 + g_{uv\theta}^* uv + \frac{g_{vv\theta}^*}{2} v^2 \end{pmatrix},$$

here all the partial derivatives with the superscript stars represent the values of the corresponding partial derivatives when $\theta = \theta_T$. Set

$$a'_{11}(\theta_T) = \frac{(c - 1)m^2 - 2(c + 1)m\theta_T + (c + 1)\theta_T^2}{cm(m - \theta_T)^2}, \quad a'_{12}(\theta_T) = -1, \\ a'_{21}(\theta_T) = -\frac{c + 1}{cm}, \quad a'_{22}(\theta_T) = 0$$

and

$$a''_{11}(\theta_T) = \frac{-2m}{c(m - \theta_T)^3}.$$

Define the second order matrices M_1 and M_2 by

$$M_1 = \begin{pmatrix} a'_{11}(\theta_T) & a'_{12}(\theta_T) \\ a'_{21}(\theta_T) & a'_{22}(\theta_T) \end{pmatrix}, \quad M_2 = \begin{pmatrix} a''_{11}(\theta_T) & 0 \\ 0 & 0 \end{pmatrix}.$$

Then the linear operator $L(\theta)$ can be approximately decomposed into the following form:

$$L(\theta) = L_T + (\theta - \theta_T)M_1 + (\theta - \theta_T)^2M_2 + O((\theta - \theta_T)^3), \tag{3.7}$$

where

$$L_T = \begin{pmatrix} a_{11}(\theta_T) + d_{11} \left(\frac{\partial^2}{\partial x^2} + \frac{\partial^2}{\partial y^2} \right) & a_{12}(\theta_T) + d_{12} \left(\frac{\partial^2}{\partial x^2} + \frac{\partial^2}{\partial y^2} \right) \\ a_{21}(\theta_T) + d_{21} \left(\frac{\partial^2}{\partial x^2} + \frac{\partial^2}{\partial y^2} \right) & a_{22}(\theta_T) + d_{22} \left(\frac{\partial^2}{\partial x^2} + \frac{\partial^2}{\partial y^2} \right) \end{pmatrix}.$$

Now we let

$$\frac{\partial}{\partial t} = \epsilon \frac{\partial}{\partial T_1} + \epsilon^2 \frac{\partial}{\partial T_2} + O(\epsilon^3). \tag{3.8}$$

Substitute the decomposition formulas (3.4)–(3.8) into (3.2), and compare the coefficients of different orders of ϵ , it is obtained that

$$L_T \begin{pmatrix} u_1 \\ v_1 \end{pmatrix} = 0, \tag{3.9}$$

$$L_T \begin{pmatrix} u_2 \\ v_2 \end{pmatrix} = \frac{\partial}{\partial T_1} \begin{pmatrix} u_1 \\ v_1 \end{pmatrix} - \theta_1 M_1 \begin{pmatrix} u_1 \\ v_1 \end{pmatrix} - N_2(\theta_T), \tag{3.10}$$

and

$$\begin{aligned} L_T \begin{pmatrix} u_3 \\ v_3 \end{pmatrix} &= \frac{\partial}{\partial T_1} \begin{pmatrix} u_2 \\ v_2 \end{pmatrix} + \frac{\partial}{\partial T_2} \begin{pmatrix} u_1 \\ v_1 \end{pmatrix} - \theta_1 M_1 \begin{pmatrix} u_2 \\ v_2 \end{pmatrix} \\ &\quad - \theta_1^2 M_2 \begin{pmatrix} u_1 \\ v_1 \end{pmatrix} - \theta_2 M_1 \begin{pmatrix} u_1 \\ v_1 \end{pmatrix} - N_{31}(\theta_T) - \theta_1 N_{32}(\theta_T). \end{aligned} \tag{3.11}$$

Define respectively Φ and Ψ by and

$$\Phi = -\frac{a_{12}(\theta_T) - k_T^2 d_{12}}{a_{11}(\theta_T) - k_T^2 d_{11}} = -\frac{a_{22}(\theta_T) - k_T^2 d_{22}}{a_{21}(\theta_T) - k_T^2 d_{21}}$$

and

$$\Psi = -\frac{a_{11}(\theta_T) - k_T^2 d_{11}}{a_{21}(\theta_T) - k_T^2 d_{21}} = -\frac{a_{12}(\theta_T) - k_T^2 d_{12}}{a_{22}(\theta_T) - k_T^2 d_{22}}.$$

Then the general solution of the linear homogeneous Eq. (3.9) can be expressed as the form

$$\begin{pmatrix} u_1 \\ v_1 \end{pmatrix} = \begin{pmatrix} \Phi \\ 1 \end{pmatrix} \left(\sum_{j=1}^3 W_j e^{i\mathbf{k}_j \cdot \mathbf{r}} + \sum_{j=1}^3 \bar{W}_j e^{-i\mathbf{k}_j \cdot \mathbf{r}} \right), \tag{3.12}$$

where W_j are the amplitudes corresponding to the modes of $e^{i\mathbf{k}_j \cdot \mathbf{r}}$ ($j = 1, 2, 3$). Here \mathbf{k}_j ($j = 1, 2, 3$) are called as wave vectors such that $|\mathbf{k}_j| = k_T$ and $\mathbf{k}_1 + \mathbf{k}_2 + \mathbf{k}_3 = \mathbf{0}$, see [18, 32].

According to the Fredholm solvability condition [19], Eq. (3.10) has a nontrivial solution if the vector function at the right end of Eq. (3.10) is orthogonal to the eigenfunction of operator L_T^+ corresponding to zero eigenvalue, where

$$L_T^+ = \begin{pmatrix} a_{11}(\theta_T) + d_{11} \left(\frac{\partial^2}{\partial x^2} + \frac{\partial^2}{\partial y^2} \right) & a_{21}(\theta_T) + d_{21} \left(\frac{\partial^2}{\partial x^2} + \frac{\partial^2}{\partial y^2} \right) \\ a_{12}(\theta_T) + d_{12} \left(\frac{\partial^2}{\partial x^2} + \frac{\partial^2}{\partial y^2} \right) & a_{22}(\theta_T) + d_{22} \left(\frac{\partial^2}{\partial x^2} + \frac{\partial^2}{\partial y^2} \right) \end{pmatrix}.$$

Notice that the zero eigenvector of L_T^+ is

$$\begin{pmatrix} 1 \\ \Psi \end{pmatrix} \left(\sum_{j=1}^3 W_j e^{i\mathbf{k}_j \cdot \mathbf{r}} + \sum_{j=1}^3 \bar{W}_j e^{-i\mathbf{k}_j \cdot \mathbf{r}} \right). \tag{3.13}$$

Let

$$\begin{pmatrix} F_u \\ F_v \end{pmatrix} = \frac{\partial}{\partial T_1} \begin{pmatrix} u_1 \\ v_1 \end{pmatrix} - \theta_1 M_1 \begin{pmatrix} u_1 \\ v_1 \end{pmatrix} - N_2(\theta_T).$$

Then when $(F_u, F_v)^T$ and (3.13) are orthogonal, we have

$$(1, \Psi) \begin{pmatrix} F_u^j \\ F_v^j \end{pmatrix} = 0, \quad j = 1, 2, 3, \tag{3.14}$$

where F_u^j and F_v^j are the coefficients of $e^{i\mathbf{k}_j \cdot \mathbf{r}}$ ($j = 1, 2, 3$) in F_u and F_v . Denote

$$H_1^* = \Phi a'_{11}(\theta_T) + a'_{12}(\theta_T) + \Psi(\Phi a'_{21}(\theta_T) + a'_{22}(\theta_T)), \tag{3.15}$$

and

$$H_2(\theta) = 2[h_1(\theta) + \Psi h_2(\theta)], \tag{3.16}$$

where

$$h_1(\theta) = \frac{f_{uu}(\theta)}{2}\Phi^2 + f_{uv}(\theta)\Phi + \frac{f_{vv}(\theta)}{2},$$

and

$$h_2(\theta) = \frac{g_{uu}(\theta)}{2}\Phi^2 + g_{uv}(\theta)\Phi + \frac{g_{vv}(\theta)}{2}.$$

Then from (3.14) we can get the equations about amplitudes W_j are

$$\begin{aligned} (\Phi + \Psi) \frac{\partial W_1}{\partial T_1} &= \theta_1 H_1^* W_1 + H_2^* \bar{W}_2 \bar{W}_3 \\ (\Phi + \Psi) \frac{\partial W_2}{\partial T_1} &= \theta_1 H_1^* W_2 + H_2^* \bar{W}_1 \bar{W}_3 \\ (\Phi + \Psi) \frac{\partial W_3}{\partial T_1} &= \theta_1 H_1^* W_3 + H_2^* \bar{W}_1 \bar{W}_2, \end{aligned} \tag{3.17}$$

where H_2^* denotes the value of H_2 at $\theta = \theta_T$.

In the next, we need to solve Eq. (3.10). To ensure the convergence of W_j ($j = 1, 2, 3$) in (3.17), the higher order terms like $e^{2\mathbf{i}k_j \cdot \mathbf{r}}$ and $e^{\mathbf{i}(k_i - k_j) \cdot \mathbf{r}}$ should be considered in u_2 and v_2 . Let

$$\begin{aligned} \begin{pmatrix} A_0 \\ B_0 \end{pmatrix} &= \begin{pmatrix} -2 \frac{a_{22}(\theta_T)h_1 - a_{12}(\theta_T)h_2}{a_{11}(\theta_T)a_{22}(\theta_T) - a_{12}(\theta_T)a_{21}(\theta_T)} \\ -2 \frac{a_{11}(\theta_T)h_2 - a_{21}(\theta_T)h_1}{a_{11}(\theta_T)a_{22}(\theta_T) - a_{12}(\theta_T)a_{21}(\theta_T)} \end{pmatrix} \\ \begin{pmatrix} A_1 \\ B_1 \end{pmatrix} &= \begin{pmatrix} -\frac{(a_{22}(\theta_T) - 4d_{22}k_T^2)h_1 - (a_{12}(\theta_T) - 4d_{12}k_T^2)h_2}{(a_{11}(\theta_T) - 4d_{11}k_T^2)(a_{22}(\theta_T) - 4d_{22}k_T^2) - (a_{12}(\theta_T) - 4d_{12}k_T^2)(a_{21}(\theta_T) - 4d_{21}k_T^2)} \\ -\frac{(a_{11}(\theta_T) - 4d_{11}k_T^2)h_2 - (a_{21}(\theta_T) - 4d_{21}k_T^2)h_1}{(a_{11}(\theta_T) - 4d_{11}k_T^2)(a_{22}(\theta_T) - 4d_{22}k_T^2) - (a_{12}(\theta_T) - 4d_{12}k_T^2)(a_{21}(\theta_T) - 4d_{21}k_T^2)} \end{pmatrix} \\ \begin{pmatrix} A_2 \\ B_2 \end{pmatrix} &= \begin{pmatrix} -2 \frac{(a_{22}(\theta_T) - 3d_{22}k_T^2)h_1 - (a_{12}(\theta_T) - 3d_{12}k_T^2)h_2}{(a_{11}(\theta_T) - 3d_{11}k_T^2)(a_{22}(\theta_T) - 3d_{22}k_T^2) - (a_{12}(\theta_T) - 3d_{12}k_T^2)(a_{21}(\theta_T) - 3d_{21}k_T^2)} \\ -2 \frac{(a_{11}(\theta_T) - 3d_{11}k_T^2)h_2 - (a_{21}(\theta_T) - 3d_{21}k_T^2)h_1}{(a_{11}(\theta_T) - 3d_{11}k_T^2)(a_{22}(\theta_T) - 3d_{22}k_T^2) - (a_{12}(\theta_T) - 3d_{12}k_T^2)(a_{21}(\theta_T) - 3d_{21}k_T^2)} \end{pmatrix}. \end{aligned}$$

Then the solution of Eq. (3.10) is given by

$$\begin{aligned} \begin{pmatrix} u_2 \\ v_2 \end{pmatrix} &= \begin{pmatrix} U_0 \\ V_0 \end{pmatrix} + \sum_{j=1}^3 \begin{pmatrix} U_j \\ V_j \end{pmatrix} e^{i\mathbf{k}_j \cdot \mathbf{r}} + \sum_{j=1}^3 \begin{pmatrix} U_{jj} \\ V_{jj} \end{pmatrix} e^{2i\mathbf{k}_j \cdot \mathbf{r}} \\ &+ \sum_{\substack{i,j=1 \\ i < j}}^3 \begin{pmatrix} U_{ij} \\ V_{ij} \end{pmatrix} e^{i(\mathbf{k}_i - \mathbf{k}_j) \cdot \mathbf{r}} + c.c., \end{aligned} \tag{3.18}$$

in which

$$\begin{pmatrix} U_0 \\ V_0 \end{pmatrix} = \begin{pmatrix} A_0^* \\ B_0^* \end{pmatrix} (|W_1^2| + |W_2^2| + |W_3^2|), \quad U_j = \Phi V_j,$$

and

$$\begin{pmatrix} U_{jj} \\ V_{jj} \end{pmatrix} = \begin{pmatrix} A_1^* \\ B_1^* \end{pmatrix} W_j^2, \quad \begin{pmatrix} U_{ij} \\ V_{ij} \end{pmatrix} = \begin{pmatrix} A_2^* \\ B_2^* \end{pmatrix} W_i \bar{W}_j,$$

here A_i^* and B_i^* ($j = 0, 1, 2$) denote the values of A_i and B_i ($j = 0, 1, 2$) when $\theta = \theta_T$.

Set

$$\begin{aligned} \begin{pmatrix} \tilde{F}_u \\ \tilde{F}_v \end{pmatrix} &= \frac{\partial}{\partial T_1} \begin{pmatrix} u_2 \\ v_2 \end{pmatrix} + \frac{\partial}{\partial T_2} \begin{pmatrix} u_1 \\ v_1 \end{pmatrix} - \theta_1 M_1 \begin{pmatrix} u_2 \\ v_2 \end{pmatrix} \\ &- \theta_1^2 M_2 \begin{pmatrix} u_1 \\ v_1 \end{pmatrix} - \theta_2 M_1 \begin{pmatrix} u_1 \\ v_1 \end{pmatrix} - N_{31}(\theta_T) - \theta_1 N_{32}(\theta_T), \end{aligned} \tag{3.19}$$

and \tilde{F}_u^j and \tilde{F}_v^j denote separately the coefficients of $e^{i\mathbf{k}_j \cdot \mathbf{r}}$ ($j = 1, 2, 3$) in \tilde{F}_u and \tilde{F}_v . Then, the orthogonality of $(\tilde{F}_u, \tilde{F}_v)^T$ and (3.13) gives

$$(1, \Psi) \begin{pmatrix} \tilde{F}_u^j \\ \tilde{F}_v^j \end{pmatrix} = 0, \quad j = 1, 2, 3.$$

Let

$$H_3^* = \Phi a'_{11}(\theta_T) + a'_{12}(\theta_T) + \Psi(\Phi a'_{21}(\theta_T) + a'_{22}(\theta_T)), \quad H_4^* = 2(h_3^* + \Psi h_4^*),$$

where

$$h_3^* = \frac{f_{uu\theta}^*}{2} \Phi^2 + f_{uv\theta}^* \Phi + \frac{f_{vv\theta}^*}{2}, \quad h_4^* = \frac{g_{uu\theta}^*}{2} \Phi^2 + g_{uv\theta}^* \Phi + \frac{g_{vv\theta}^*}{2}.$$

Furthermore, define $G_1(\theta)$ and $G_2(\theta)$ by

$$\begin{aligned}
 G_1(\theta) = & (A_0 + A_1)[f_{uu}(\theta)\Phi + f_{uv}(\theta)] + (B_0 + B_1)[f_{uv}(\theta)\Phi + f_{vv}(\theta)] \\
 & + \frac{f_{uuu}(\theta)}{2}\Phi^3 + \frac{3f_{uuv}(\theta)}{2}\Phi^2 + \frac{3f_{uvv}(\theta)}{2}\Phi + \frac{f_{vvv}(\theta)}{2} \\
 & + \Psi[(A_0 + A_1)[g_{uu}(\theta)\Phi + g_{uv}(\theta)] + (B_0 + B_1)[g_{uv}(\theta)\Phi + g_{vv}(\theta)] \\
 & + \frac{g_{uuu}(\theta)}{2}\Phi^3 + \frac{3g_{uuv}(\theta)}{2}\Phi^2 + \frac{3g_{uvv}(\theta)}{2}\Phi + \frac{g_{vvv}(\theta)}{2},
 \end{aligned} \tag{3.20}$$

and

$$\begin{aligned}
 G_2(\theta) = & (A_0 + A_2)[f_{uu}(\theta)\Phi + f_{uv}(\theta)] + (B_0 + B_2)[f_{uv}(\theta)\Phi + f_{vv}(\theta)] \\
 & + f_{uuu}(\theta)\Phi^3 + 3f_{uuv}(\theta)\Phi^2 + 3f_{uvv}(\theta)\Phi + f_{vvv}(\theta) \\
 & + \Psi[(A_0 + A_2)[g_{uu}(\theta)\Phi + g_{uv}(\theta)] + (B_0 + B_2)[g_{uv}(\theta)\Phi + g_{vv}(\theta)] \\
 & + g_{uuu}(\theta)\Phi^3 + 3g_{uuv}(\theta)\Phi^2 + 3g_{uvv}(\theta)\Phi + g_{vvv}(\theta).
 \end{aligned} \tag{3.21}$$

Then putting (3.12) and (3.18) into (3.11), we can obtain the equations about amplitudes V_j and W_j are as follows:

$$\begin{aligned}
 (\Phi + \Psi) \left(\frac{\partial V_1}{\partial T_1} + \frac{\partial W_1}{\partial T_2} \right) = & H_1^*(\theta_1 V_1 + \theta_2 W_1) + H_2^*(\bar{V}_2 \bar{W}_3 + \bar{V}_3 \bar{W}_2) + \theta_1^2 H_3^* W_1 \\
 & + [G_1^* | W_1 |^2 + G_2^*(| W_2 |^2 + | W_3 |^2)] W_1 + \theta_1 H_4^* \bar{W}_2 \bar{W}_3 \\
 (\Phi + \Psi) \left(\frac{\partial V_2}{\partial T_1} + \frac{\partial W_2}{\partial T_2} \right) = & H_1^*(\theta_1 V_2 + \theta_2 W_2) + H_2^*(\bar{V}_3 \bar{W}_1 + \bar{V}_1 \bar{W}_3) + \theta_1^2 H_3^* W_2 \\
 & + [G_1^* | W_2 |^2 + G_2^*(| W_1 |^2 + | W_3 |^2)] W_2 + \theta_1 H_4^* \bar{W}_1 \bar{W}_3 \\
 (\Phi + \Psi) \left(\frac{\partial V_3}{\partial T_1} + \frac{\partial W_3}{\partial T_2} \right) = & H_1^*(\theta_1 V_3 + \theta_2 W_3) + H_2^*(\bar{V}_1 \bar{W}_2 + \bar{V}_2 \bar{W}_1) + \theta_1^2 H_3^* W_3 \\
 & + [G_1^* | W_3 |^2 + G_2^*(| W_1 |^2 + | W_2 |^2)] W_3 + \theta_1 H_4^* \bar{W}_1 \bar{W}_2,
 \end{aligned} \tag{3.22}$$

where $G_1^* = G_1(\theta_T)$ and $G_2^* = G_2(\theta_T)$.

Now in system (3.1) let

$$\begin{pmatrix} u \\ v \end{pmatrix} = \sum_{j=1}^3 \begin{pmatrix} A_j \\ B_j \end{pmatrix} \left(\sum_{j=1}^3 W_j e^{ik_j \cdot r} + \sum_{j=1}^3 \bar{W}_j e^{-ik_j \cdot r} \right) + \dots .$$

Then it follows from [18, 30] that $A_j = \Phi B_j (j = 1, 2, 3)$ and the amplitudes A_j can be expanded as

$$A_j = \epsilon W_j + \epsilon^2 V_j + O(\epsilon^3), j = 1, 2, 3.$$

According to the decomposition (3.8), the partial derivative of amplitudes A_j ($j = 1, 2, 3$) with respect to time t has the form

$$\frac{\partial A_j}{\partial t} = \epsilon^2 \frac{\partial W_j}{\partial T_1} + \epsilon^3 \frac{\partial W_j}{\partial T_2} + \epsilon^3 \frac{\partial V_j}{\partial T_1} + O(\epsilon^4).$$

Let $H(\theta)$ be given by

$$H(\theta) = \Phi(a_{11}(\theta) - a_{11}(\theta_T)) + a_{12}(\theta) - a_{12}(\theta_T) + \Psi[\Phi(a_{21}(\theta) - a_{21}(\theta_T)) + a_{22}(\theta) - a_{22}(\theta_T)]$$

and

$$\mu = \frac{H(\theta)}{\Phi + \Psi}, \quad h = \frac{H_2(\theta)}{\Phi + \Psi}, \quad g_1 = -\frac{G_1(\theta)}{\Phi + \Psi}, \quad g_2 = -\frac{G_2(\theta)}{\Phi + \Psi},$$

where $H_2(\theta)$, $G_1(\theta)$ and $G_2(\theta)$ are given respectively by (3.16) and (3.21). It follows from (3.17) and (3.22) that the amplitude equations of model (1.4) near (u_*, v_*) are

$$\begin{aligned} \frac{\partial A_1}{\partial t} &= \mu A_1 + h \bar{A}_2 \bar{A}_3 - [g_1 |A_1|^2 + g_2 (|A_2|^2 + |A_3|^2)] A_1, \\ \frac{\partial A_2}{\partial t} &= \mu A_2 + h \bar{A}_1 \bar{A}_3 - [g_1 |A_2|^2 + g_2 (|A_1|^2 + |A_3|^2)] A_2, \\ \frac{\partial A_3}{\partial t} &= \mu A_3 + h \bar{A}_1 \bar{A}_2 - [g_1 |A_3|^2 + g_2 (|A_1|^2 + |A_2|^2)] A_3. \end{aligned} \tag{3.23}$$

4 Classification and Stability of Turing Patterns

In the present section, we discuss the existence and stability of Turing patterns arising near the Turing threshold in system (1.5) through the amplitude equations obtained in the previous section. A stable Turing pattern corresponds to a stable steady state solution of Eq. (3.23). Since each amplitude in (3.23) can be expressed into the function of a mode $\rho_i = |A_i|$ and a phase angle φ_i , one can know that A_j can be written into $A_j = \rho_j e^{i\varphi_j}$ ($j = 1, 2, 3$). Putting $A_j = \rho_j e^{i\varphi_j}$ ($j = 1, 2, 3$) into Eq.(3.23) and separating the real and the imaginary parts, we have the following equations

$$\begin{cases} \frac{\partial \varphi}{\partial t} = -h \frac{\rho_1^2 \rho_2^2 + \rho_1^2 \rho_3^2 + \rho_2^2 \rho_3^2}{\rho_1 \rho_2 \rho_3} \sin \varphi, \\ \frac{\partial \rho_1}{\partial t} = \mu \rho_1 + h \rho_2 \rho_3 \cos \varphi - g_1 \rho_1^3 - g_2 (\rho_2^2 + \rho_3^2) \rho_1, \\ \frac{\partial \rho_2}{\partial t} = \mu \rho_2 + h \rho_1 \rho_3 \cos \varphi - g_1 \rho_2^3 - g_2 (\rho_1^2 + \rho_3^2) \rho_2, \\ \frac{\partial \rho_3}{\partial t} = \mu \rho_3 + h \rho_1 \rho_2 \cos \varphi - g_1 \rho_3^3 - g_2 (\rho_1^2 + \rho_2^2) \rho_3, \end{cases} \tag{4.1}$$

where $\varphi = \varphi_1 + \varphi_2 + \varphi_3$. According to [18, 19], we know that system (4.1) has the following four kinds of stationary solutions when $g_1, g_2 > 0$.

(1) The stationary state

$$\rho_1 = \rho_2 = \rho_3 = 0$$

is stable if $\mu < 0 \triangleq \mu_2$ and unstable for $\mu > \mu_2$.

(2) The stripe pattern solution

$$S : \rho_1 = \sqrt{\frac{\mu}{g_1}}, \rho_2 = \rho_3 = 0$$

exists when $\mu > 0$. The stripe solution $(\sqrt{\frac{\mu}{g_1}}, 0, 0)$ is stable for

$$\mu > \frac{h^2 g_1}{(g_2 - g_1)^2} \triangleq \mu_3$$

and unstable for $0 < \mu < \mu_3$.

(3) The hexagon pattern solutions

$$H_0 : \rho_1 = \rho_2 = \rho_3 = \frac{|h| + \sqrt{h^2 + 4(g_1 + 2g_2)\mu}}{2(g_1 + 2g_2)},$$

$$H_\pi : \rho_1 = \rho_2 = \rho_3 = \frac{|h| - \sqrt{h^2 + 4(g_1 + 2g_2)\mu}}{2(g_1 + 2g_2)},$$

exist when

$$\mu > \frac{-h^2}{4(g_1 + 2g_2)} \triangleq \mu_1.$$

The solution H_0 is stable only for

$$\mu < \frac{h^2(2g_1 + g_2)}{(g_2 - g_1)^2} \triangleq \mu_4,$$

while H_π is always unstable.

(4) The mixed state

$$\rho_1 = \frac{|h|}{g_2 - g_1}, \rho_2 = \rho_3 = \sqrt{\frac{\mu - g_1 \rho_1^2}{g_1 + g_2}},$$

exists when $g_2 > g_1$, $\mu > g_1 \rho_1^2$ and it is always unstable.

It is easy to know that under the condition $g_1, g_2 > 0$, the critical value $\mu_k (k = 1, 2, 3, 4)$ have the relationship $\mu_1 < \mu_2 < \mu_3 < \mu_4$. The curves of S , H_0 and H_π against μ are demonstrated in Fig. 3 and we can see that when $\mu_1 < \mu < \mu_2$, both the uniform stationary solution and the hexagonal pattern H_0 are stable; when

Fig. 3 Chart of stationary solutions of system (4.1) in μ - ρ plane. The solid line shows that the stationary solution of (4.1) is stable and the dotted one shows that it is unstable

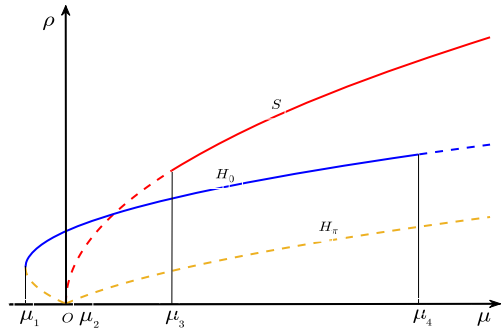


Table 1 Range of μ with respect to different values of θ

h	g_1	g_2	μ_1	μ_2	μ_3	μ_4	μ	range of μ	
0.345	-0.2029	0.1846	0.4431	-0.0096	0	0.1139	0.5010	0.0209 $\mu_1 < \mu_2 < \mu < \mu_3 < \mu_4$	
0.36	-0.1157	0.5292	1.1954	-0.0011	0	0.0160	0.0680	0.0168 $\mu_1 < \mu_2 < \mu_3 < \mu < \mu_4$	
0.376	-0.0267	0.7061	1.4660	-0.000049	145	0	0.00087428	0.0036	0.0092 $\mu_1 < \mu_2 < \mu_3 < \mu_4 < \mu$

$\mu_2 < \mu < \mu_3$, only the hexagonal pattern H_0 is stable; when $\mu_3 < \mu < \mu_4$, both the stripe pattern S and hexagonal pattern H_0 are stable; when $\mu > \mu_4$, only the stripe is stable. In addition, when $\mu > \mu_4$, the hexagonal pattern H_π is always unstable.

5 Numerical Simulations for Pattern Formations

In this section, we shall give some numerical simulations in order to verify the theoretical results obtained in Sects. 2 and 3. To carry out our numerical simulations, initial conditions in system (1.5) is taken as the random ones, $L_x = L_y = 200$, and system (1.5) is numerically integrated by using the finite difference approximation of spatial derivatives and the explicit Euler method of time derivative, in which the time step is 1/100. Set the parameters in system (1.5) as $d_{11} = 0.5, d_{12} = 0.5, d_{21} = 1.45, d_{22} = 1.5, m = 0.8, c = 2$. Then in this case $\theta_H = 0.2667$ and $\theta_T = 0.3892$. Take $\theta = 0.345, \theta = 0.36$ and $\theta = 0.376$ respectively. Then the values for $\mu_k (k = 1, 2, 3, 4)$ and μ are set in the Table 1.

When $\theta = 0.345$, μ is between μ_2 and μ_3 . According to the previous theoretical analysis, system (1.5) will have a stable spot pattern and the stable H_0 hexagon pattern, see Fig. 4. According to Fig. 4d, except for the yellow spots, the prey population is mainly distributed in the blue square area. The numerical simulation shows that the numerical results are consistent with the theoretical ones.

When $\theta = 0.36$, it can be seen that $\mu \in (\mu_3, \mu_4)$ and hence the stripe and H_0 hexagon patterns of system (1.5) are stable, see Fig. 5. It is shown that spot patterns and stripe patterns occur simultaneously and they compete each other. The dynamics of the model shows the transition from spot patterns to stripe patterns growth, that is, spot patterns decay and stripe patterns occur.

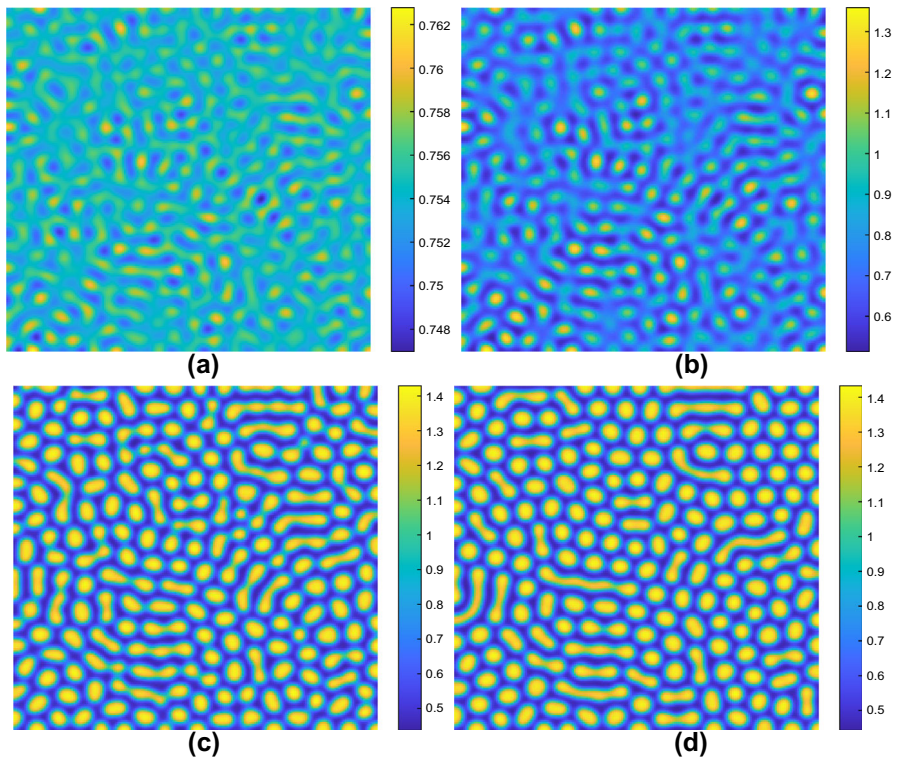


Fig. 4 Simulation diagrams of the prey species of system (1.5) with $d_{11} = 0.5$, $d_{12} = 0.5$, $d_{21} = 1.45$, $d_{22} = 1.5$, $m = 0.8$, $c = 2$ and $\theta = 0.345$ at different instants. **a** $t = 200$, **b** $t = 400$, **c** $t = 1000$, **d** $t = 2000$

When θ is selected as 0.376, one can find from Table 1 that $\mu > \mu_4$ and so only the stripe patterns are stable. The numerical results show that the final pattern is the stripe pattern, see Fig. 6. It can be found that the labyrinth pattern occupies the entire spatial area.

6 Conclusions

Although reaction–diffusion systems with self-diffusion can more reasonably predict the development of some species than the associated ODE models, under some particular situations cross-diffusion among species cannot still be omitted. Consequently, we regarded a classical two-species predator–prey reaction–diffusion system with the linear self-diffusion and cross-diffusion and subject to homogeneous Neumann boundary condition on a planar rectangle domain in this paper.

It has been found in [29] that only random freedom diffusion in the classical predator–prey system with the Holling-II type functional response and subject to homogeneous Neumann boundary condition on a bounded domain with a smooth boundary doesn't affect the stability of the constant coexistence equilibrium. Whether

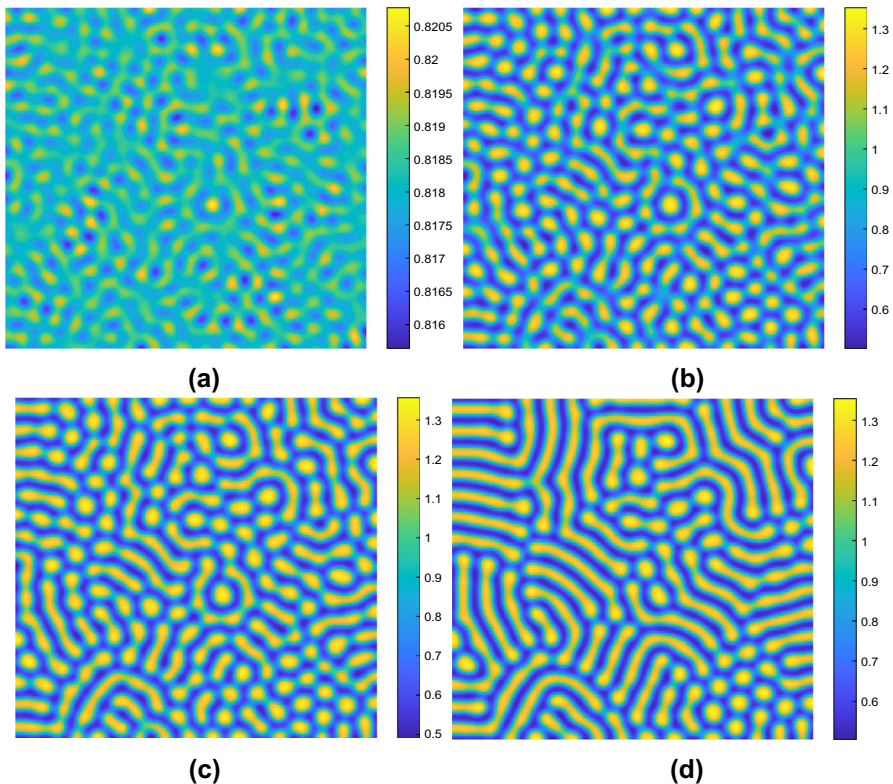


Fig. 5 Simulation diagrams of the prey species of system (1.5) with $d_{11} = 0.5$, $d_{12} = 0.5$, $d_{21} = 1.45$, $d_{22} = 1.5$, $m = 0.8$, $c = 2$ and $\theta = 0.36$ at different instants. **a** $t = 200$, **b** $t = 600$, **c** $t = 1000$, **d** $t = 2000$

or not the cross-diffusion can bring out more complicated dynamical behaviors in reaction–diffusion systems is an important and interesting subject. Here, we explored mainly the effect of cross-diffusion on dynamical behaviors of system in [29] and it was shown that the occurrence of linear cross-diffusion can arise more complicated dynamical behaviors such as various Turing patterns.

The effect of linear cross-diffusion on dynamical behaviors of model (1.5) have been concerned in [25], however, they gave only numerical simulations for the associated phenomena but not the detailed theoretical analysis. Therefore, the classification and stability of Turing patterns of system (1.5) near the unique constant coexistence equilibrium cannot be determined. The main contribution of this paper is that the classification and stability of Turing patterns of (1.5) near the unique constant coexistence equilibrium were gave in detail.

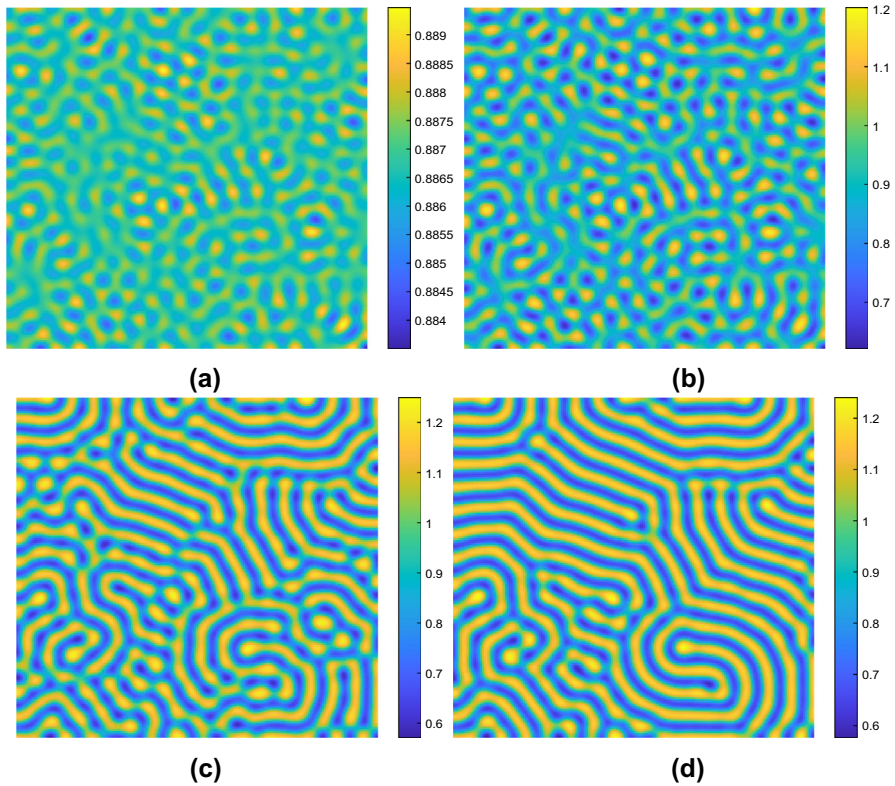


Fig. 6 Simulation diagrams of the prey species of system (1.5) with $d_{11} = 0.5$, $d_{12} = 0.5$, $d_{21} = 1.45$, $d_{22} = 1.5$, $m = 0.8$, $c = 2$ and $\theta = 0.376$ at different instants. **a** $t = 400$, **b** $t = 1000$, **c** $t = 2000$, **d** $t = 4000$

Acknowledgements We would like to express our grateful thanks to the reviewers for their careful reading and helpful comments of the manuscript

Author Contributions Xiang-Ping Yan and Tong-Jie Yang wrote the manuscript text and completed all the computations in the manuscript. Xiang-Ping Yan checked the correction of all the formula and revised all the problems like grammas, computations etc. Cun-Hua Zhang completed all the figures in the manuscript. All authors reviewed the manuscript.

Declarations

Conflict of interest The authors declare no competing interests.

References

1. Bentout, S., Djilali, S., Atangana, A.: Bifurcation analysis of an age-structured prey–predator model with infection developed in prey. *Math. Methods Appl. Sci.* **45**, 1189–1208 (2022)
2. Bentout, S., Djilali, S., Ghanbari, B.: Backward, Hopf bifurcation in a heroin epidemic model with treat age. *Int. J. Model. Simul. Sci. Comput.* **12**, 2150018 (2021)

3. Bentout, S., Djilali, S., Kuniya, T., Wang, J.-L.: Mathematical analysis of a vaccination epidemic model with nonlocal diffusion. *Math. Methods Appl. Sci.* **46**, 10970–10994 (2023)
4. Boudjema, I., Djilali, S.: Turing-Hopf bifurcation in Gauss-type model with cross diffusion and its application. *Nonlinear Stud.* **25**, 665–687 (2018)
5. Chen, S.-S., Shi, J.-P., Wei, J.-J.: The effect of delay on a diffusive predator-prey system with Holling type-II predator functional response. *Commun. Pure Appl. Anal.* **12**, 481–501 (2013)
6. Chen, M.-X., Wu, R.-C., Chen, L.-P.: Spatiotemporal patterns induced by Turing and Turing-Hopf bifurcations in a predator-prey system. *Appl. Math. Comput.* **380**, 125300 (2020)
7. Cheng, K.-S.: Uniqueness of a limit cycle for a predator-prey system. *SIAM J. Math. Anal.* **12**, 541–548 (1981)
8. Djilali, S.: Pattern formation of a diffusive predator-prey model with herd behavior and nonlocal prey competition. *Math. Methods Appl. Sci.* **43**, 2233–2250 (2020)
9. Djilali, S.: Threshold asymptotic dynamics for a spatial age-dependent cell-to-cell transmission model with nonlocal disperse. *Discrete Contin. Dyn. Syst. Ser. B* **28**, 4108–4143 (2023)
10. Djilali, S., Bentout, S.: Pattern formations of a delayed diffusive predator-prey model with predator harvesting and prey social behavior. *Math. Methods Appl. Sci.* **44**, 9128–9142 (2021)
11. Guin, L.-N.: Spatial patterns through Turing instability in a reaction-diffusion predator-prey model. *Math. Comput. Simul.* **109**, 174–185 (2015)
12. Hsu, S.-B.: On global stability of a predator-prey system. *Math. Biosci.* **39**, 1–10 (1978)
13. Hu, G.-P., Li, X.-L.: Turing patterns of a predator-prey model with a modified Leslie-Gower term and cross-diffusions. *Int. J. Biomath.* **5**, 1250060 (2012)
14. Iida, M., Mimura, M., Ninomiya, H.: Diffusion, cross-diffusion and competitive interaction. *J. Math. Biol.* **53**, 617–641 (2006)
15. Li, Y.-X., Liu, H., Wei, Y.-M., Ma, M.: Turing pattern of a reaction-diffusion predator-prey model with weak Allee effect and delay. *J. Phys. Conf. Ser.* **1707**, 012025 (2020)
16. Mezouaghi, A., Djilali, S., Bentout, S., Biroud, K.: Bifurcation analysis of a diffusive predator-prey model with prey social behavior and predator harvesting. *Math. Methods Appl. Sci.* **45**, 718–731 (2022)
17. Murray, J.-D.: *Mathematical Biology II*. Springer, Heidelberg (1993)
18. Ouyang, Q., Gunaratne, G.H., Swinney, H.L.: Rhombic patterns: broken hexagonal symmetry. *Chaos* **3**, 707–711 (1993)
19. Ou, Y.-X.: *Nonlinear Science and the Pattern Dynamics Introduction*. Peking University Press, Beijing (2010)
20. Peng, R., Shi, J.-P.: Non-existence of non-constant positive steady states of two Holling type-II predator-prey systems: Strong interaction case. *J. Differ. Equ.* **247**, 866–886 (2009)
21. Song, Y.-L., Tang, X.-S.: Stability, steady-state bifurcations, and Turing patterns in a predator-prey model with herd behavior and prey-taxis. *Stud. Appl. Math.* **139**, 371–404 (2017)
22. Tang, X.-S., Song, Y.-L.: Cross-diffusion induced spatiotemporal patterns in a predator-prey model with herd behavior. *Nonlinear Anal. Real World Appl.* **24**, 36–49 (2015)
23. Turing, A.-M.: The chemical basis of morphogenesis. *Bull. Math. Biol.* **237**, 37–72 (1952)
24. Vanag, V., Epstein, I.: Cross-diffusion and pattern formation in reaction-diffusion systems. *Phys. Chem. Chem. Phys.* **11**, 897–912 (2009)
25. Wang, Q.-F., Peng, Y.-H.: Turing instability and pattern induced by cross-diffusion in a predator-prey system. *J. Shanghai Normal Univ. (Nat. Sci.)* **47**, 331–337 (2018)
26. Wu, J.-H.: *Theory and Applications of Partial Functional Differential Equations*. Springer, New York (1996)
27. Yan, X.-P., Zhang, C.-H.: Stability and Turing instability in a diffusive predator-prey system with Beddington-DeAngelis functional response. *Nonlinear Anal. Real World Appl.* **20**, 1–13 (2014)
28. Yang, B.: Pattern formation in a diffusive ratio-dependent Holling-Tanner predator-prey model with Smith growth. *Discrete Dyn. Nat. Soc.* **1**, 87–118 (2013)
29. Yi, F.-Q., Wei, J.-J., Shi, J.-P.: Bifurcation and spatio-temporal patterns in a homogeneous diffusive predator-prey system. *J. Differ. Equ.* **246**, 1944–1977 (2009)
30. Yuan, S.-L., Xu, C.-Q., Zhang, T.-H.: Spatial dynamics in a predator-prey model with herd behavior. *Chaos* **23**, 33102–33102 (2013)
31. Zhang, J.-F., Li, W.-T., Yan, X.-P.: Hopf bifurcation and Turing instability in spatial homogeneous and inhomogeneous predator-prey models. *Appl. Math. Comput.* **218**, 1883–1893 (2011)
32. Zhou, Y., Yan, X.-P., Zhang, C.-H.: Turing patterns induced by self-diffusion in a predator-prey model with schooling behavior in predator and prey. *Nonlinear Dyn.* **105**, 3731–3747 (2021)

Publisher's Note Springer Nature remains neutral with regard to jurisdictional claims in published maps and institutional affiliations.

Springer Nature or its licensor (e.g. a society or other partner) holds exclusive rights to this article under a publishing agreement with the author(s) or other rightsholder(s); author self-archiving of the accepted manuscript version of this article is solely governed by the terms of such publishing agreement and applicable law.